

Confined Concrete—Its Application in R.C. Beams and Frames

K. T. SUNDARA RAJA IYENGAR*
PRAKASH DESAYI*
K. NAGI REDDY†

Stress-strain characteristics of concrete confined in steel binders have been determined. A new factor "confinement index" has been introduced for a quantitative measure of the confinement and using these results a "stress-block" has been developed. Tests have been made on simply supported reinforced concrete beams with spiral binder confinement and analysed on the basis of the proposed stress-block. Tests have also been made on reinforced concrete portal frames and continuous beams with spiral binder confinement at sections of possible plastic hinge formation. An analysis of these tests indicates that a full redistribution of moments has taken place at ultimate.

NOTATION

<p>A_{st} area of longitudinal tension steel</p> <p>A_{sc} area of longitudinal compression steel</p> <p>b breadth of the rectangular beam</p> <p>C compressive force in concrete</p> <p>C_s force in compression steel</p> <p>C_i confinement index</p> <p>d effective depth of the concrete beam</p> <p>d' depth of A_{sc} below the compression edge of the beam</p> <p>E_{st} modulus of elasticity of tension steel</p> <p>E_{sc} modulus of elasticity of compression steel</p> <p>f_a average stress of the stress block</p> <p>f_c compressive stress corresponding to the strain ϵ_c</p> <p>f_c' ultimate compressive strength of plain (unconfined) concrete cylinder or prism</p> <p>\bar{f}_c ultimate strength of a confined concrete specimen</p> <p>f_y yield stress of tension steel; or 0.2 per cent proof stress or yield stress of steel wire used as binder when defining C_i</p> <p>f_y' yield stress of compression steel</p> <p>f_s stress in steel</p> <p>f_1, f_2 stresses as defined in the stress blocks (figures 3 and 4)</p> <p>f_1 $0.9f_c'$</p> <p>f_2 $0.9\bar{f}_c$</p> <p>kf_1 stress in the stress-block of confined concrete for a strain of $\beta\epsilon_1$</p> <p>k_1 f_2/f_1</p> <p>l span</p> <p>M bending moment</p> <p>M_u ultimate moment</p> <p>m E_{st}/E_c where $E_c = 0.9f_c'/0.0012$</p> <p>n neutral axis depth factor</p> <p>nd depth of neutral axis</p> <p>p tension steel ratio = A_{st}/bd</p> <p>p' compression steel ratio = A_{sc}/bd</p> <p>p_b volumetric ratio, i.e. ratio of the volume of binder to the volume of confined concrete</p> <p>\bar{p}_b value of p_b when the pitch of binder is equal to the least lateral dimension of the specimen</p>	<p>r d'/d</p> <p>W load on the beam or frame</p> <p>W_y yield load</p> <p>W_u ultimate load</p> <p>X distance of the centre of gravity of the stress-block from the stress axis</p> <p>ϵ_c strain in concrete cylinder or prism, or extreme fibre strain in compression concrete of a section in flexure</p> <p>ϵ_c' strain at maximum stress of plain concrete cylinder or prism</p> <p>$\epsilon_1, \epsilon_2, \epsilon_3, \epsilon_4$ strains as defined in the stress-blocks (figures 3 and 4)</p> <p>ϵ_{sc} strain in compression steel</p> <p>ϵ_{st} strain in tension steel</p> <p>ϵ_y yield strain of tension steel</p> <p>ϵ_y' yield strain of compression steel</p> <p>α ϵ_c/ϵ_1 in the plain concrete stress-block</p> <p>α_1 ϵ_2/ϵ_1 in the plain concrete stress-block</p> <p>β ϵ_c/ϵ_1 in the case of confined concrete stress-block</p> <p>β_1 ϵ_3/ϵ_1 in the case of confined concrete stress-block</p> <p>γ ϵ_c/ϵ_3 in the case of confined concrete stress-block</p> <p>γ_1 ϵ_4/ϵ_3 in the case of confined concrete stress-block</p> <p>χ curvature</p> <p>δ deflection</p>
--	--

INTRODUCTION

REINFORCED concrete structures, unlike steel structures, tend to fail in a relatively brittle manner as the deformation capacity of concrete is limited. The non-linear moment-curvature diagram of a reinforced concrete section reaches a maximum moment and the moment begins to decrease soon after the maximum is reached. In an indeterminate reinforced concrete structure, the highly stressed critical section reaches first its maximum moment under increasing load; as the load is still further

* Department of Civil Engineering, Indian Institute of Science, Bangalore, India.

† Department of Civil Engineering, Regional Engineering College, Warangal (A.P.), India.

increased, the moment at the highly stressed section starts decreasing while the moments at other sections are increasing. This situation leads to considerable complexity in the analysis of indeterminate concrete structures. The moment adaptability of a reinforced concrete indeterminate structure is limited and it decreases rapidly with increasing yield strength of the reinforcement and with higher steel ratios. This drawback could be compensated to some extent by providing compression steel; this however will offset to some extent the economic gain in using high strength steels[1]. A possible method of retaining the economic benefits of using high strength steels coupled with the adaptation of inelastic design, appears to lie in improving the ductility of concrete in compression. Ductility will be also beneficial in accommodating the effect of foundation settlements, volume changes, etc. Improvement in ductility makes concrete a more efficient building material, increases its usefulness for structures subjected to dynamic loads and also makes the ultimate load analysis and design of indeterminate reinforced concrete structures as simple as those of steel structures.

It is possible to improve the ductility of concrete if the material can be prevented from disruption and falling apart into pieces when compressed to its ultimate capacity. This can be done by providing suitable confinement to the concrete under compression. Investigations in which concrete specimens were compressed and at the same time subjected to lateral hydrostatic pressure indicate an increased compressibility and strength of such specimens[2, 3]. The lateral pressure provides a confinement and presents a lateral support for the bulging specimen and prevents the disruption under longitudinal compression. A practicable method of confining concrete in structural members appears to be the use of steel binders (spirals or stirrups) around the periphery of concrete in compression. Knowing that in a framed structure under load there are certain critical sections at which largest moments occur, provision of steel binders to confine the concrete in compression at these critical sections will improve the deformable capacity of the section and hence will permit a complete redistribution of moments at ultimate. Thus, a reinforced or prestressed concrete frame having steel binder confinement at critical sections, will overcome most of the disadvantages resulting from the poor ductile property of concrete.

As a result of the many beneficial effects of confining concrete in steel binders, investigations on this aspect of concrete strength and deformation have been receiving considerable attention. Studies of Richart *et al.*[4] deal with the increase in strength

of circular concrete columns due to provision of spiral steel binders while those of Martin[5] concern with the stress-strain properties of spirally prestressed concrete cylinders. Chan[6], Szulczynski and Sozen[7], Rüsck and Stöckl[8], Roy and Sozen[9, 10], Bertero and Felippa[11], and Soliman and Yu[12] deal with confinements provided by means of circular/rectangular ties with tests conducted on plain/reinforced concrete specimens under axial/eccentric loading. The properties determined in compression tests have been used in the analysis of reinforced concrete beams having concrete confined by web stirrups by Chan[6], Rüsck and Stöckl[8], Soliman and Yu[12], Baker and Amarkone[13] and Corley[14]. Test results of Bertero and Felippa[11] show that stirrups and compression steel increase the rotation capacity of reinforced concrete sections. Tests by Base[15], Base and Read[16], Warwaruk and Ward[17] and Nawy *et al.*[18] demonstrate the large rotations which can be realized in reinforced and prestressed concrete beam sections by introducing circular and square spirals to confine concrete.

While a few methods are found available for the flexural analysis of beams having rectangular stirrup confinement[6, 8, 12–14] similar methods for the flexural analysis when confinement is due to circular or square spirals appear to be lacking. Hence, a project comprising of the determination of stress-strain curves of concrete confined in steel binders, development of suitable stress-blocks for the flexural analysis of reinforced concrete sections with steel binder confinement, and a theoretical and experimental study of determinate and indeterminate reinforced concrete beams and frames was undertaken. This paper presents briefly some of the results of this study and more details of experimental observations are included elsewhere[19].

STRENGTH AND DEFORMATION OF CONCRETE CONFINED IN STEEL BINDERS

In order to make a proper analysis of the flexure of reinforced concrete sections with spiral steel confinement, the basic data needed are the stress-blocks which can be deduced from the stress-strain characteristics of such concrete. Stress-strain curves were determined in uniaxial compression on 150×300 mm cylinders, 100×200 mm cylinders, $150 \times 150 \times 300$ mm prisms and $100 \times 100 \times 200$ mm prisms in a strain-rate control test. Along with plain concrete specimens, cylinders with circular spiral steel binders were cast and tested. For spiral wire, two types of steel viz., 5 mm dia. high-tensile steel wire and 6.5 mm dia. mild steel wire were used and the pitch of the spiral was varied between

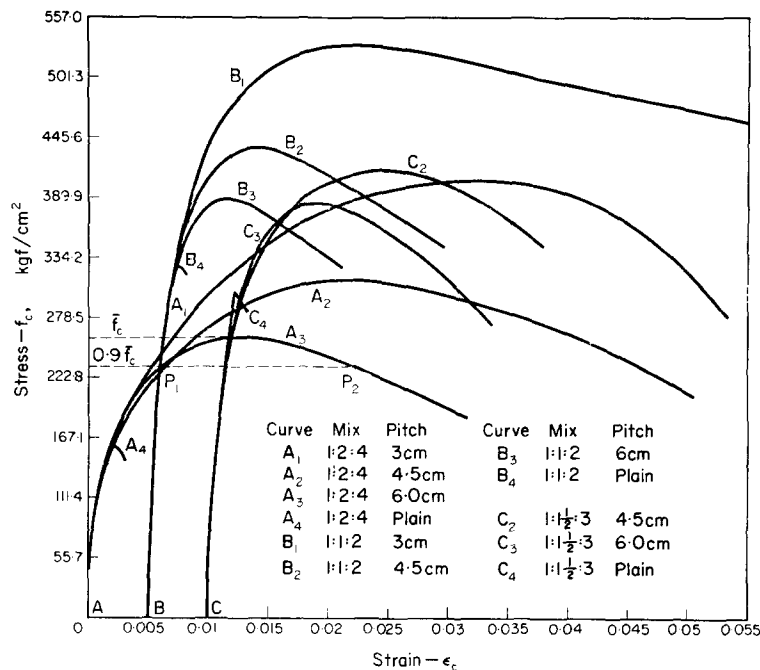


Fig. 1. Stress-strain curves of 100 x 200 mm concrete cylinders confined with circular spiral 5 mm dia. hard steel wire.

30 and 100 mm. Concrete of three different mixes viz., 1:2:4, 1:1.5:3 and 1:1:2 were used. For a given size of specimen, mix, diameter of wire and pitch, at least three specimens were cast and tested and the average taken. Thus a total of about 240 specimens were tested in the investigation.

Compression tests were made in a hydraulically operated universal testing machine of 100 tonne capacity. An arrangement consisting of four dial gauges fitted at four diametrically opposite points between two square frames which could be attached to the test specimen was used for measurement of strains. Figure 1 shows some typical stress-strain curves determined in the study.

CONFINEMENT INDEX AND THE INFLUENCE OF CONFINEMENT

In order to have a quantitative measure of the confinement offered by the binders, it is necessary to have a single expression which takes into account all the dimensional and strength parameters of the confined and confining media. For this purpose, the volumetric ratio (p_b) has been used in literature[6]. In this investigation it was felt that the use of p_b only as a measure of confinement is insufficient as it does not include the strength properties. The analysis of the test results showed that a parameter "confinement index" (C_i) is a better representation of the confinement and is defined

$$C_i = (p_b - \bar{p}_b) \frac{f_y}{f'_c} \tag{1}$$

Confinement is known to increase the strength and deformation capacity of concrete. This can be observed in the typical stress-strain curves of figure 1. From the stress-strain curves, data of the stress and strain at maximum, and strains at 90 and 85 per cent of the maximum in the descending portion of the stress-strain curve, were analysed for determining the influence of confinement on the strength and deformation of concrete. The following results were obtained for cylindrical specimens having circular spiral confinement:

$$\frac{\bar{f}_c}{f'_c} = 1 + 2.30(p_b - \bar{p}_b) \frac{f_y}{f'_c} \tag{2}$$

$$\frac{\bar{\epsilon}_c}{\epsilon'_c} = 1 + 23.0(p_b - \bar{p}_b) \frac{f_y}{f'_c} \tag{3}$$

$$\frac{\bar{\epsilon}_{0.9}}{\epsilon'_c} = 1.5 + 41.5(p_b - \bar{p}_b) \frac{f_y}{f'_c} \tag{4}$$

$$\frac{\bar{\epsilon}_{0.85}}{\epsilon'_c} = 1.8 + 46.5(p_b - \bar{p}_b) \frac{f_y}{f'_c} \tag{5}$$

A study of the mechanics of the action of steel binders indicated a close similarity of the confinement offered by lateral hydrostatic pressure with that of the circular spiral binder. These results and a more detailed report on the stress-strain characteristics of concrete confined in steel binders have been recently published[20].

DEVELOPMENT OF STRESS BLOCKS

For the development of stress-blocks required in the flexural analysis of reinforced concrete sections

with compression concrete confined in circular spirals, equation (2) given above and the data of strains at 90 per cent of the maximum stress have been utilized.

Considering a typical stress-strain curve of a confined concrete specimen (say, curve A3 in figure 1), let points P_1 and P_2 on this curve correspond to 90 per cent of the maximum stress in the ascending and descending portions respectively. Figure 2 has been prepared using the coordinates of such points P_1 and P_2 of all the stress-strain curves (determined on specimens with circular spiral binder) and equation (2). Experimental points are omitted in figure 2 and the best fitting straight lines only indicated. The following details explain figure 2:

- AA_1 Coordinates of points P_1 of figure 1 for confinement due to circular spiral binder.
- BB_1 Coordinates of points P_2 of figure 1 for confinement due to circular spiral binder.
- GG_1 Influence of circular spiral confinement on the strength. Refer to equation 2.
- $OABC$ Stress block for concrete not confined.

$OAD_1E_1F_1$ Stress-block for concrete confined in circular spiral binder giving a confinement of $C_i = OH$.

In the analysis, when using the stress block in figure 2, for the value of f'_c , the strength of 150×300 mm plain cylinder is used so that the procedure will be in accordance with the usual practice adopted for the case of no confinement.

EQUATIONS FOR MOMENT AND CURVATURE

With the stress-blocks determined, equations for moment and curvature of reinforced concrete sections were written down using the statical equilibrium and strain compatibility conditions. The usual assumptions viz., (1) steel behaves as an ideal elastic-plastic material, (2) tensile strength of concrete is negligible and (3) plane sections before bending remain plane after bending, were used in the analysis.

Figures 3, 4 and 5 give the strain and stress distribution across a section subjected to flexure and Tables 1, 2 and 3 give the resulting equations for the depth of neutral axis, resisting moment and curvature.

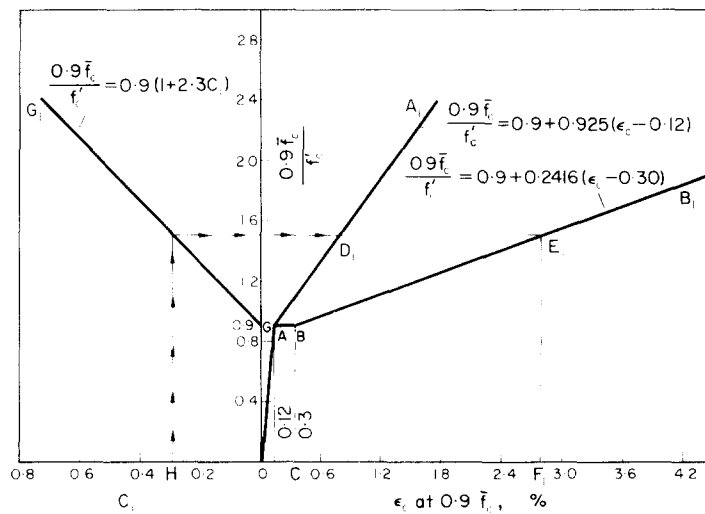


Fig. 2. Stress-blocks for confined and unconfined concretes (Circular spiral confinement).

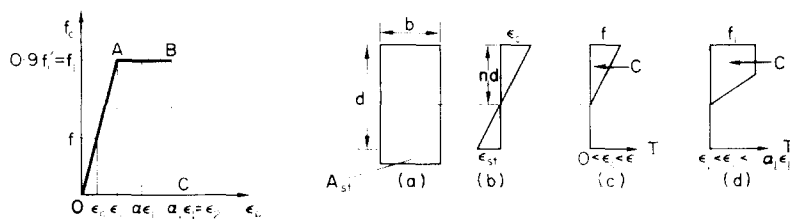


Fig. 3. Stress-block for unconfined concrete and the variation of strains and stresses on a r.c. section in bending.

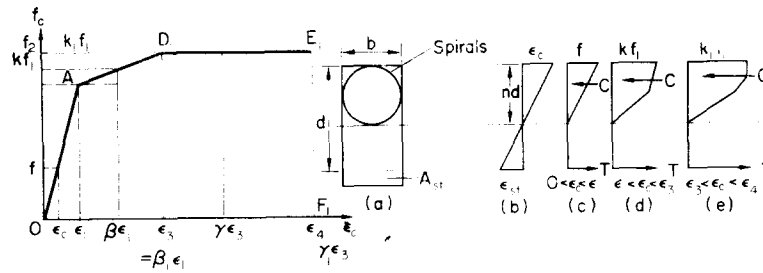


Fig. 4. Stress-block for confined concrete and the variation of strains and stresses on a r.c. section in bending.

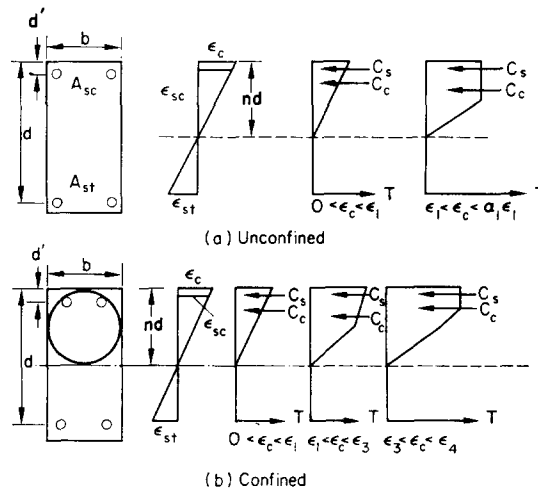


Fig. 5. Stresses and strains across a doubly reinforced section in bending.

Table 1. Equations for nd and $M/bd^2f'_c$ for singly reinforced sections without confinement.

Extreme fibre strain	Steel strain	Neutral axis depth factor "n" to be determined from	Resisting moment factor $M/bd^2f'_c$ given by
$0 < \epsilon_c < \epsilon_1$	$\epsilon_{st} < \epsilon_y$	$n^2/(1-n) = \frac{f}{f_a} pm$	$n^2 \frac{f_a}{f'_c} \frac{\bar{X}}{\epsilon_c} + p \frac{f_s}{f'_c} (1-n)$
	$\epsilon_{st} > \epsilon_y$	$n = \frac{pf_y}{f_a}$	$n^2 \frac{f_a}{f'_c} \frac{\bar{X}}{\epsilon_c} + p \frac{f_y}{f'_c} (1-n)$
where $f_a = f/2, \bar{X}/\epsilon_c = \frac{2}{3}$			
$\epsilon_1 < \epsilon_c < \epsilon_2$ ($\epsilon_c = \alpha\epsilon_1$)	$\epsilon_{st} < \epsilon_y$	$n^2/(1-n) = \frac{f_1}{f_a} \alpha pm$	$n^2 \frac{f_a}{f'_c} \frac{\bar{X}}{\epsilon_c} + p \frac{f_s}{f'_c} (1-n)$
	$\epsilon_{st} > \epsilon_y$	$n = \frac{pf_y}{f_a}$	$n^2 \frac{f_a}{f'_c} \frac{\bar{X}}{\epsilon_c} + p \frac{f_y}{f'_c} (1-n)$
where $f_a = \frac{2\alpha-1}{2\alpha} f_1, \frac{\bar{X}}{\epsilon_c} = \frac{3\alpha^2-1}{3(2\alpha-1)}$			

Note: $\chi d = \epsilon_c/n$.

Table 2. Equations for nd and M/bd^2f_c' for singly reinforced sections with confinement.

Extreme fibre strain	Steel strain	Neutral axis depth factor "n" to be determined from	Resistance moment factor M/bd^2f_c' given by
Same as that in Table 1			
$0 < \varepsilon_c < \varepsilon_1$	$\varepsilon_{st} < \varepsilon_y$	$n^2/(1-n) = \frac{f_1}{f_a} p m$	$n^2 \frac{f_a}{f_c'} \frac{\bar{X}}{\varepsilon_c} + p \frac{f_s}{f_c'} (1-n)$
	$\varepsilon_{st} > \varepsilon_y$	$n = p \frac{f_y}{f_a}$	$n^2 \frac{f_a}{f_c'} \frac{\bar{X}}{\varepsilon_c} + p \frac{f_y}{f_c'} (1-n)$
Where $f_a = f_1 \left[\frac{\beta(k+1)-k}{2\beta} \right]$, $\frac{\bar{X}}{\varepsilon_c} = \frac{1}{3\beta} \left[\frac{\beta^2(2k+1)-\beta(k-1)-k}{\beta(k+1)-k} \right]$			
$\varepsilon_1 < \varepsilon_c < \varepsilon_3$ ($\varepsilon_c = \beta\varepsilon_1$)	$\varepsilon_{st} < \varepsilon_y$	$n^2/(1-n) = \frac{f_1}{f_a} p \gamma \beta_1 m$	$n^2 \frac{f_a}{f_c'} \frac{\bar{X}}{\varepsilon_c} + p \frac{f_s}{f_c'} (1-n)$
	$\varepsilon_{st} > \varepsilon_y$	$n = p \frac{f_y}{f_a}$	$n^2 \frac{f_a}{f_c'} \frac{\bar{X}}{\varepsilon_c} + p \frac{f_y}{f_c'} (1-n)$
Where $f_a = f_1 \frac{\beta_1(k_1+1)-k_1+2\beta_1k_1(\gamma-1)}{2\gamma\beta_1}$ $\frac{\bar{X}}{\varepsilon_c} = \frac{1}{3\gamma\beta_1} \frac{\beta_1^2(2k_1+1)-\beta_1(k_1-1)-k_1+3\beta_1^2k_1(\gamma^2-1)}{\beta_1(k_1+1)-k_1+2\beta_1k_1(\gamma-1)}$			
$\varepsilon_3 < \varepsilon_c < \varepsilon_4$ ($\varepsilon_c = \gamma\varepsilon_3$)	$\varepsilon_{st} < \varepsilon_y$	$n^2/(1-n) = \frac{f_1}{f_a} p \gamma \beta_1 m$	$n^2 \frac{f_a}{f_c'} \frac{\bar{X}}{\varepsilon_c} + p \frac{f_s}{f_c'} (1-n)$
	$\varepsilon_{st} > \varepsilon_y$	$n = p \frac{f_y}{f_a}$	$n^2 \frac{f_a}{f_c'} \frac{\bar{X}}{\varepsilon_c} + p \frac{f_y}{f_c'} (1-n)$

Note: $\chi d = \varepsilon_c/n$.Table 3. Equations for nd and M/bd^2f_c' for doubly reinforced sections with and without confinement.

Tension steel strain	Compression steel strain	Neutral axis depth factor "n" to be determined from	Resisting moment factor M/bd^2f_c' given by
$\varepsilon_{st} < \varepsilon_y$	$\varepsilon_{sc} < \varepsilon_y'$	$n^2 + n(p'E_{sc} + pE_{st}) \frac{\varepsilon_c}{f_a}$ $-(p'rE_{sc} + pE_{st}) \frac{\varepsilon_c}{f_a} = 0$	$n^2 \frac{f_a}{f_c'} \frac{\bar{X}}{\varepsilon_c} + \frac{p'E_{sc}\varepsilon_c}{f_c'}$ $\times \frac{(n-r)^2}{n} + \frac{pE_{st}\varepsilon_c}{f_c'} \frac{(1-n)^2}{n}$
$\varepsilon_{st} > \varepsilon_y$	$\varepsilon_{sc} < \varepsilon_y'$	$n^2 + \frac{n}{f_a} (p'E_{sc}\varepsilon_c - pf_y)$ $-p'r \frac{E_{sc}\varepsilon_c}{f_a} = 0$	$n^2 \frac{f_a}{f_c'} \frac{\bar{X}}{\varepsilon_c} + \frac{p'E_{sc}\varepsilon_c}{f_c'}$ $\times \frac{(n-r)^2}{n} + p \frac{f_y}{f_c'} (1-n)$
$\varepsilon_{st} > \varepsilon_y$	$\varepsilon_{sc} > \varepsilon_y'$	$n = \frac{1}{f_a} (pf_y - p'f_y')$	$n^2 \frac{f_a}{f_c'} \frac{\bar{X}}{\varepsilon_c} + \frac{p'f_y'}{f_c'} (n-r)$ $+ \frac{pf_y}{f_c'} (1-n)$
$\varepsilon_{st} < \varepsilon_y$	$\varepsilon_{sc} > \varepsilon_y'$	$n^2 + \frac{n}{f_a} (p'f_y' + pE_{st}\varepsilon_c)$ $- \frac{pE_{st}\varepsilon_c}{f_a} = 0$	$n^2 \frac{f_a}{f_c'} \frac{\bar{X}}{\varepsilon_c} + \frac{p'f_y'}{f_c'} (n-r)$ $+ p \frac{E_{st}\varepsilon_c}{f_c'} \frac{(1-n)^2}{n}$

Note: (1) Values of f_a and \bar{X}/ε_c to be taken for the appropriate cases from Table 1 or 2.
(2) $\chi d = \varepsilon_c/n$.

TESTS ON SIMPLY SUPPORTED BEAMS

Reinforced concrete beams of nominal size of 10×20 cm designed to fail in flexure, were tested over a simply supported span of 150 cm under symmetrical two point loading. The beams had different percentages of tension reinforcement (p ranging from 1.4 per cent to 8 per cent) and different degrees of confinement (C_i ranging from zero to 0.6) provided by circular spirals with an outer dimension of 10 cm and provided over a length equal to the flexure span plus twice the effective depth of the beam. Higher values of p , which are known to give sudden brittle failure in ordinary beams, were purposely chosen to examine the efficiency of steel binders in imparting ductile behaviour to such cases. The beams were tested in a hydraulically operated universal testing machine under a uniform rate of cross-head movement and central deflections, steel strains and rotations in the flexure span were measured. The rotations were

measured by a set up “rotation meter” the details of which may be seen in figures 6 and 7.

Figure 8 gives typical load-deflection diagrams of the tested beams with and without circular spiral binder and, from these curves, the effect of confinement in inducing ductile behaviour is obvious. Figures 9–14 show some of the beams after testing.

Moment-curvature diagrams obtained in these tests have been found to compare favourably with those determined using the proposed method of analysis (Tables 1, 2 and 3). Also the ultimate moment of 18 beams tested in this investigation, 16 beam tests of Base and Read[16] and 14 beam tests of Warwaruk and Ward[17] were found to agree satisfactorily with the ultimate moment determined from the proposed method. More details of experimental work on the simply supported beams, moment-curvature diagrams and comparison of computed and experimental ultimate moments have been presented elsewhere [21].

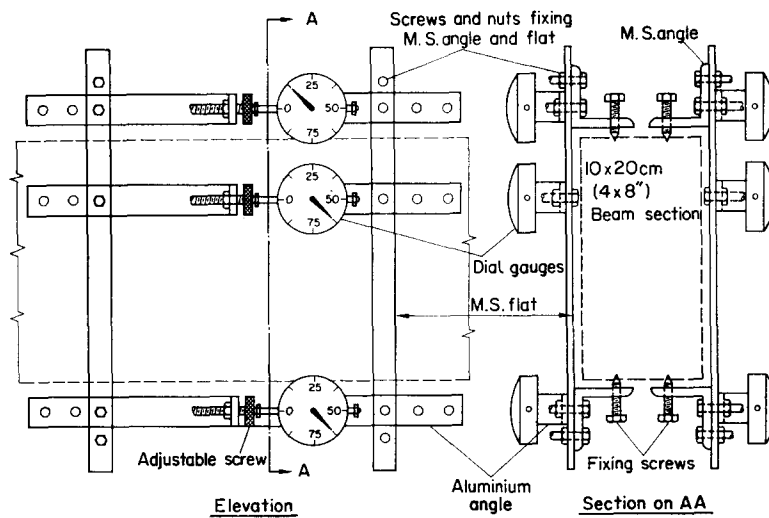


Fig. 6. Details of rotation meter.

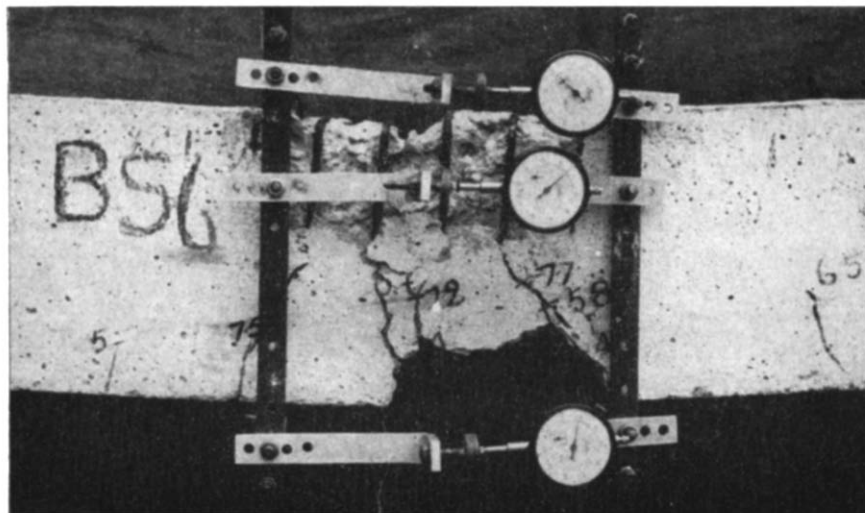


Fig. 7. Rotation meter on a beam under test.

TESTS ON PORTAL FRAMES AND CONTINUOUS BEAMS

The investigation has been aimed at a study of the ultimate strength and behaviour of reinforced concrete portal frames and continuous beams having compression concrete confined in steel spirals at locations of possible plastic hinge formation. Though the effect of confinement in improving the

ductility of concrete in compression and its use in simply supported beams had been studied to a limited extent, as already reviewed, information on its effect on indeterminate beams and frames appear to be scanty. Full or near-full redistribution of moments is known to occur in frames and beams, even without confinement when the tension reinforced used is small (less than about 2 per cent) and with/without compression steel. In these cases,

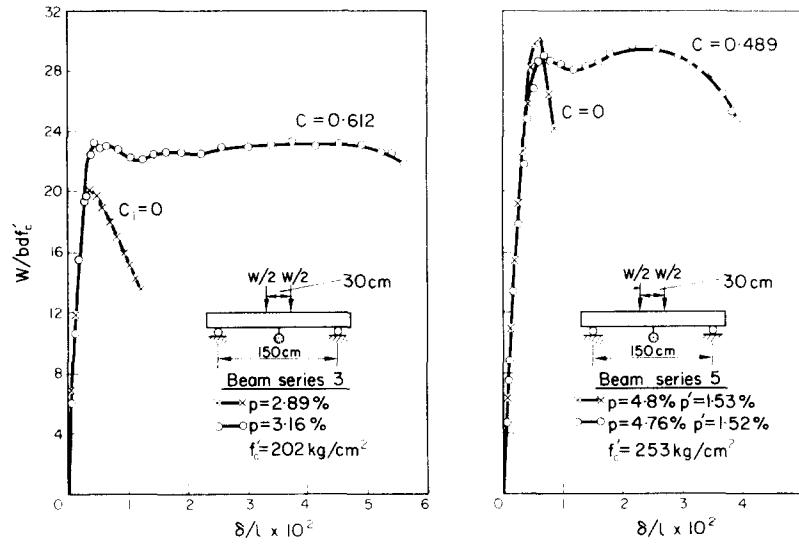


Fig. 8. Typical load-deflection diagrams of simply supported beams.

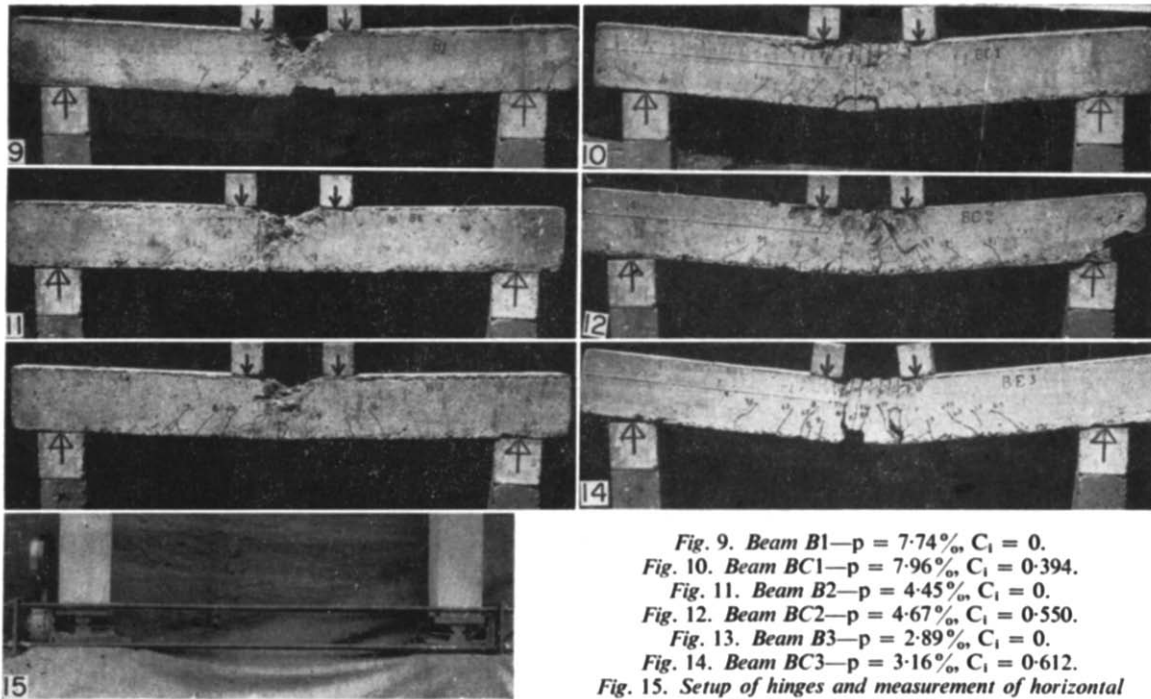


Fig. 9. Beam B1— $p = 7.74\%$, $C_1 = 0$.
 Fig. 10. Beam BC1— $p = 7.96\%$, $C_1 = 0.394$.
 Fig. 11. Beam B2— $p = 4.45\%$, $C_1 = 0$.
 Fig. 12. Beam BC2— $p = 4.67\%$, $C_1 = 0.550$.
 Fig. 13. Beam B3— $p = 2.89\%$, $C_1 = 0$.
 Fig. 14. Beam BC3— $p = 3.16\%$, $C_1 = 0.612$.
 Fig. 15. Setup of hinges and measurement of horizontal thrust for the portal frames.

Fig. 16. A portal frame under test.

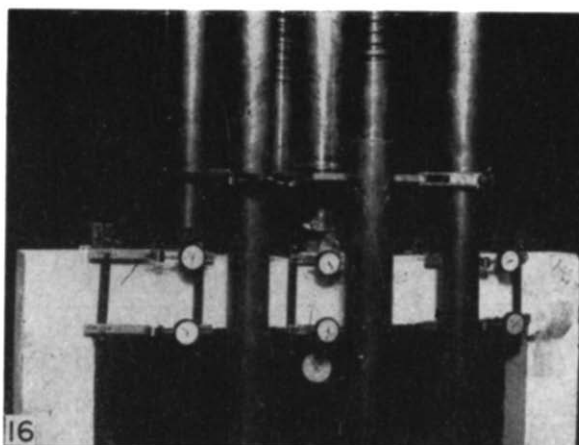


Fig. 17. Two span continuous beam under test.

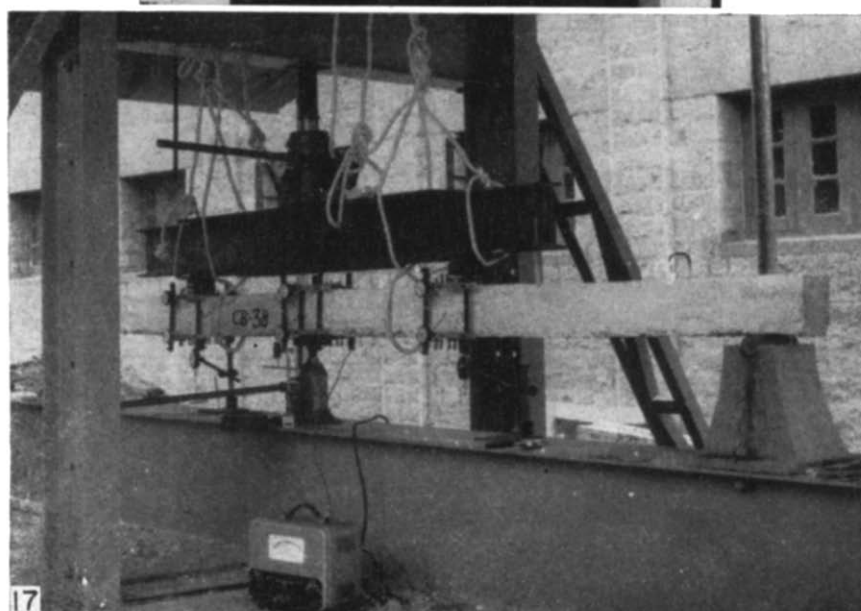


Table 4. Details of portal frames tested.

Series	Frame number	Section at	p (%)	p' (%)	f_y (kg/cm ²)	f'_c (kg/cm ²)	C_i
A	P0	Mid-transom	3.59	0.54	3465	353	0.026*
	PA0	Column top	1.49	0.52	3465	353	0.126
		Mid-transom	3.45	0.53			
B	P1	Column top	1.47	0.51	3600	328	0.056*
		Mid-transom	2.03	0.54			
	PA ₁	Column top	2.03	0.54			
		Mid-transom	2.00	0.533			
	PB ₁	Column top	2.00	0.533			
		Mid-transom	1.93	0.513			
C	P2	Column top	1.93	0.513			
		Mid-transom	3.05	0.538			
	PA ₂	Column top	3.05	0.538			
		Mid-transom	2.98	0.527			
	PB ₂	Column top	2.98	0.527			
		Mid-transom	3.04	0.537			
		Column top	3.04	0.537			

* Frames in which C_i is due to stirrups only.

Note: Yield strength of rod used for compression steel and stirrups—3050 kg/cm².

Table 5. Details of continuous beams tested.

Series	Beam number	Section at	p (%)	p' (%)	f_y (kg/cm ²)	f_c' (kg/cm ²)	C_t
1	CB1	Central support	2.74	0.730	4670	456	0.043*
		Load section	1.82	0.485			
	CB1A	Central support	2.26	0.600	4670	456	
		Load section	1.78	0.475			
	CB1B	Central support	2.32	0.617	4670	456	
		Load section	1.73	0.460			
2	CB2	Central support	4.79	0.578	3465	363	0.027*
		Load section	4.08	0.492			
	CB2A	Central support	4.72	0.570	3465	363	
		Load section	3.92	0.473			
	CB2B	Central support	4.77	0.575	3465	363	
		Load section	4.27	0.515			
3	CB3	Central support	7.53	0.635	3300	248	0.037*
		Load section	5.84	0.492			
	CB3A	Central support	6.76	0.570	3300	248	
		Load section	6.16	0.520			
	CB3B	Central support	7.25	0.612	3300	248	
		Load section	7.25	0.612			
4	CB4	Central support	2.67	0.473	3600	260	0.042*
		Load section	2.24	0.596			
	CB4A	Central support	2.67	0.473	3600	260	
		Load section	2.07	0.548			
	CB4B	Central support	2.56	0.454	3600	260	
		Load section	2.00	0.537			
5	CB5	Central support	6.90	0.555	3465	211	0.042*
		Load section	4.15	0.500			
	CB5A	Central support	6.50	0.522	3465	211	
		Load section	4.78	0.578			
	CB5B	Central support	7.48	0.600	3465	211	
		Load section	4.90	0.590			

* Beams in which C_t is due to stirrups only.

Note: Yield strength of rod used for compression steel and stirrups = 3050 kg/cm².

the usual stirrup steel provided for shear (or nominally) imparts confinement to some extent and thus assists in the redistribution processes. However, when the reinforcement used is of a higher proportion, the curvature developed under maximum moment by such sections being limited, only partial redistribution can be expected. Hence, in this test programme, study of the effect of steel binder confinement for such cases has been included in particular.

Tests have been made on two hinged portal frames having p about 1.5–3.5 per cent and two-span continuous beams having p about 1.7–7.5 per cent. The frames and beams had a nominal section of 10 × 15 cm and were provided with suitable mild steel stirrups to avoid shear failures. A total eight portal frames were tested under a concentrated load at mid-span on the transom. A total of fifteen two-span continuous beams were tested under symmetrically placed single concentrated load in each span. Nine beams were tested with the loads at 0.4 l from the central support and six beams with

loads at 0.575 l from the central support. In the first group of nine beams, the load arrangement enabled the first plastic hinge to form at the central support. For the six beams of the second group, the reinforcement over the central support was 1.5 times the reinforcement at the loading section and due to this the first plastic hinge formed at the loaded section in the span. Tables 4 and 5 show the details of the portal frames and continuous beams respectively and the strength of concrete determined by testing companion specimens.

For confinement of compression concrete, 5 mm wire steel circular spirals with pitches of 45 mm, 60 mm or 75 mm and of a length equal to about twice the effective depth were provided at the sections which are expected to develop plastic hinges at collapse. As it was found that the stirrups provided for shear also imparted some confinement, total equivalent confinement was determined for the sections and the same is included in the Tables 4 and 5. The effect of confinement due to stirrups

was determined in a manner similar to that of circular spirals but with the test results of Szulczynski and Sozen[7, 20].

The portal frames were tested in a hydraulically operated universal testing machine. Suitable arrangements (shown in figure 15) were made to provide ideal hinge supports at the bottom of the frames and to measure the horizontal thrust. Rotations at critical sections were measured by attaching the rotation meters at three sections. During testing, central deflections, rotations, steel strains etc. were measured. Figure 16 shows a part of a portal frame under test.

Continuous beams were tested on a 50-tonne capacity frame, loaded by suitable hydraulic jacks. The central reaction of these symmetrically loaded beams was measured by a hydraulic jack which was pumped level with other supports after each stage of loading. Rotations at critical sections were measured by rotation meters. During testing deflections, rotations, steel strains etc. were measured. Figure 17 shows a continuous beam under test.

BEHAVIOUR OF FRAMES AND BEAMS UNDER LOAD

The response of a frame or beam to loading is effectively illustrated by its load-deformation diagrams. Figures 18 and 19 represent some typical load-deflection diagrams of portal frames and continuous beams respectively. Figures 20 and 21 show typical load-curvature diagrams.

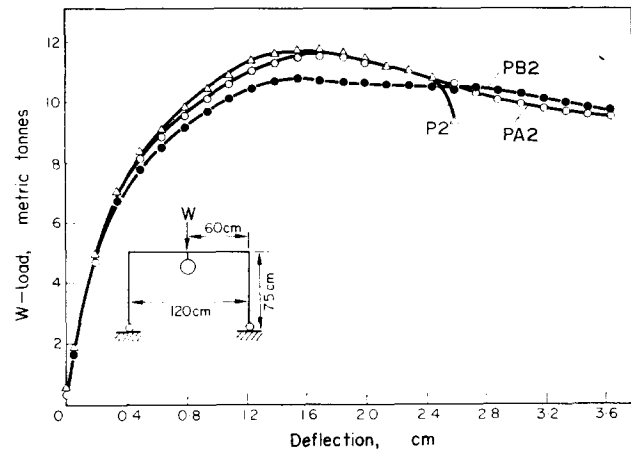


Fig. 18. Typical load-deflection diagrams of portal frames.

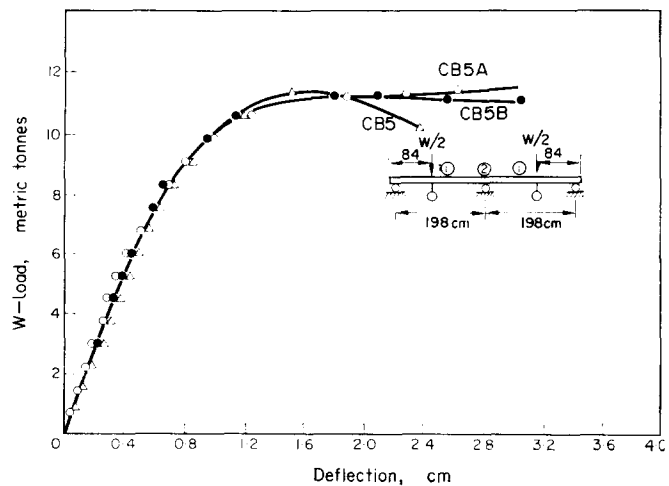


Fig. 19. Typical load-deflection diagrams of continuous beams.

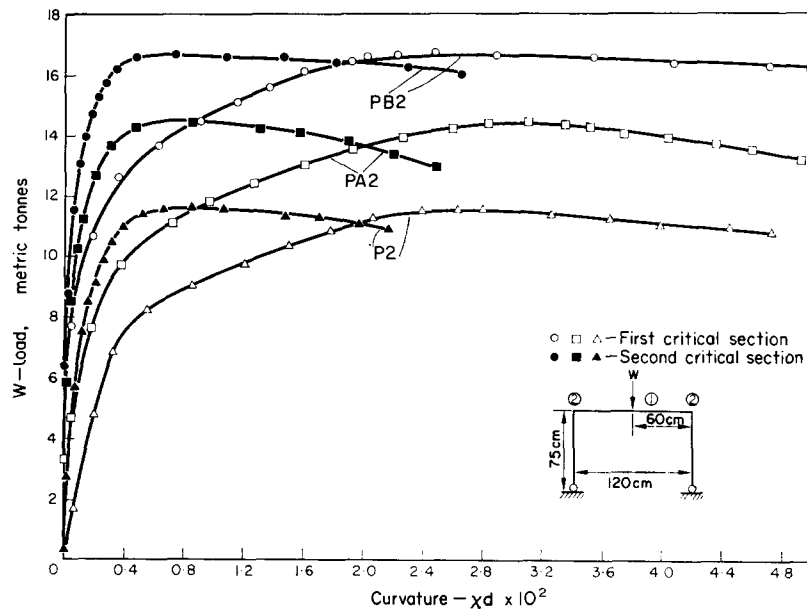


Fig. 20. Typical load-curvature diagrams of portal frames.

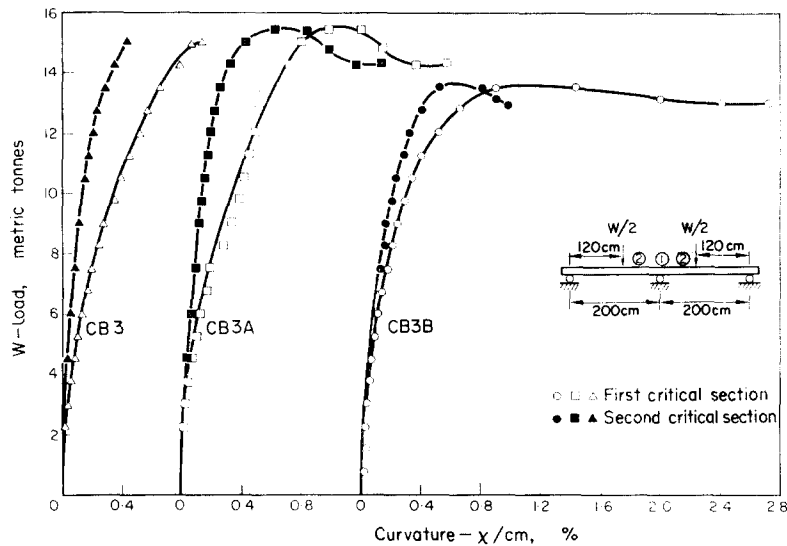


Fig. 21. Typical load-curvature diagrams of continuous beams.

It was noticed, in general, that in the early stages of loading, both confined and unconfined test specimens behaved similarly. After yielding of tension steel at the first critical section, the section was able to deform plastically at a constant moment due to the confinement of compression concrete and a plastic hinge was thus formed. After this stage, the deformations increased at a faster rate with increase of load on the specimen until the steel at the second critical section also yielded. At this stage a "mechanism" formed as the structure continued to deflect for no increase of load. The plastic behaviour of the structure depended on the magnitude of tension steel and the quantity of confinement present at the plastic hinges. As may be expected, for small values of p a plastic hinge behaviour was noticed even for small values of C_i . But when p was sufficiently large, specimens having a small value of C_i (or those without circular spirals) showed a reduced plastic behaviour than those with higher values of C_i . These points may be observed in figures 18–21.

REDISTRIBUTION OF MOMENTS

Figure 22 shows a typical plot of how the moments increased at the two critical sections of a set of portal frames. Until the yielding of tension steel at the first critical section, the moments increase as per the usual elastic behaviour. After this, the rate of increase of moment at the first critical section is reduced whereas that at the second critical section is increased. This indicates that in the later part of testing, it is the second critical section that takes up a greater share of the increasing load. This is possible because of the improved rotation capacity of the first critical section as a

result of confinement. Figures 20 and 21 clearly show the large curvatures developed at the first critical section and figure 21 shows how the presence of circular spiral confinement is beneficial in this regard when p -values are higher than ordinary.

LOADS AT YIELD AND ULTIMATE

In the redundant frames and beams the specimens become less and less rigid with the formation of plastic hinges. In the case of two-hinged portal frames and two-span continuous beams, with the yielding of tension steel at the first critical section, the specimens start yielding at an increased rate until the second plastic hinge is formed which is at the ultimate. The load at the formation of first hinge has been taken as the yield load (W_y) and that at ultimate as the ultimate load (W_u). The values of W_y and W_u have been determined analytically and compared with the experimental values.

Analytically, W_y and W_u have been determined by computing the ultimate moments of resistance of the critical sections as per the method proposed earlier (and checked by experiments on simply supported beams) using the equations in Tables 1, 2 and 3 and also assuming that the rotations required for full redistribution of moments have been developed at the plastic hinges.

Experimental value of W_u is known from the test, but the experimental value of W_y is not always quite obvious from the load-deflection diagrams. Hence the following procedure was used for determining experimental value of W_y . It is known that the kinks in the log-log straight line plots of load-deformation graphs indicate a change in the structural response[22]. As formation of a plastic

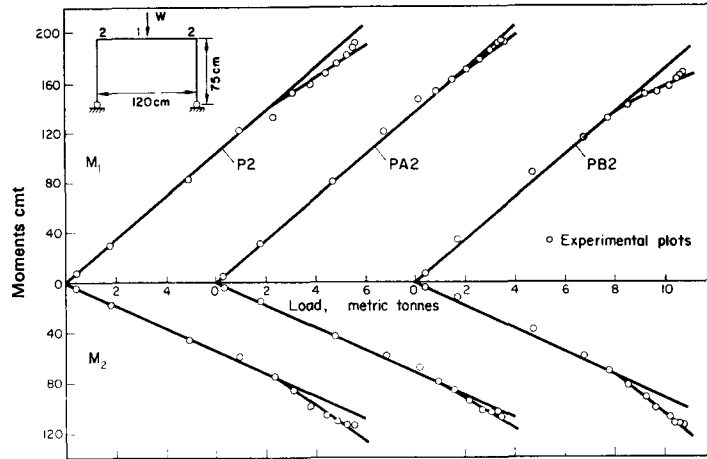


Fig. 22. Load vs. moment plot at critical sections for some portal frames.

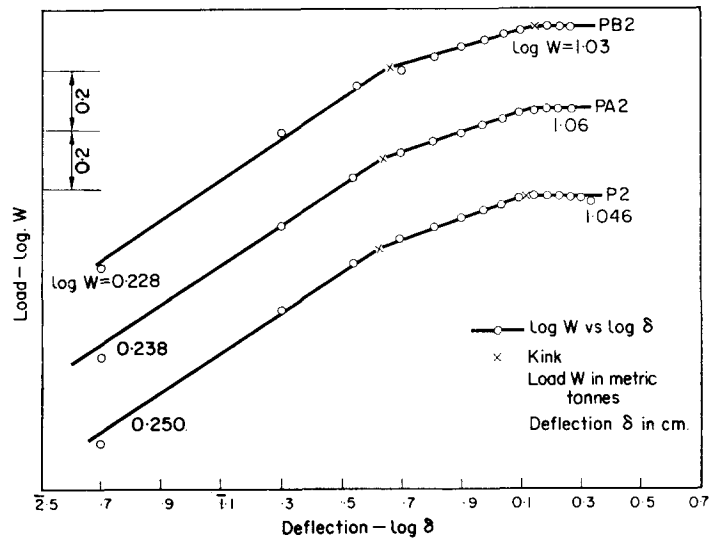


Fig. 23. Log load-log deflection plots of some portal frames.

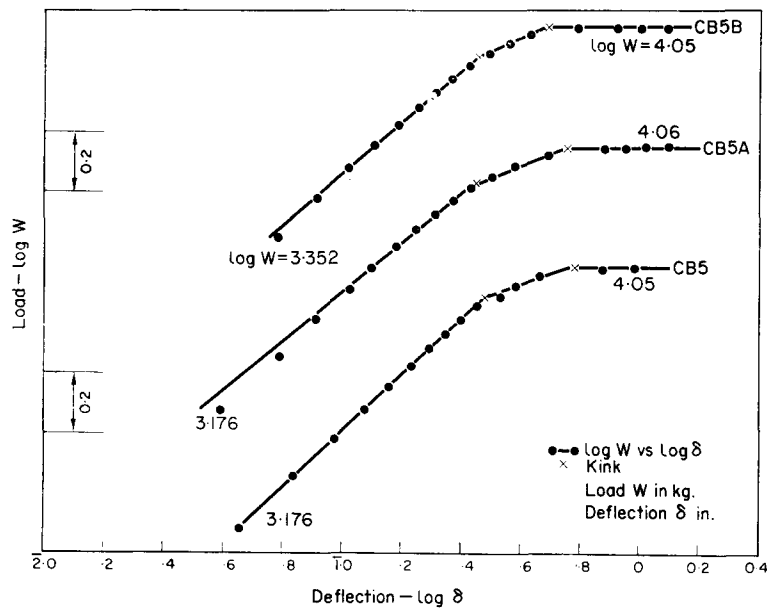


Fig. 24. Log load-log deflection plots of some continuous beams.

hinge introduces a change in the structural response of a redundant frame or beam, it was felt that a log load vs. log deflection plot might show up the stages at which these changes occurred by kinks. Hence from the observed load-deflection diagrams, log load-log deflection diagrams were prepared and it was noticed that each log-log plot consisted of three straight lines with clearly marked kinks at the meeting of the lines. (Figures 23 and 24 show typical log-log plots of portal frames and continuous beams respectively.) The initial steep line

plastic hinge was formed for these test specimens and structure carried the ultimate load, W_u .

Thus, by plotting log load-log deflection diagrams it has been possible to determine precisely the experimental values of W_y for all the test specimens. Authors feel that this is a new method which other research workers also may effectively use for determining the stages where plastic hinges form in the course of testing a reinforced concrete indeterminate structure.

Table 6 and figure 25 compare the computed and

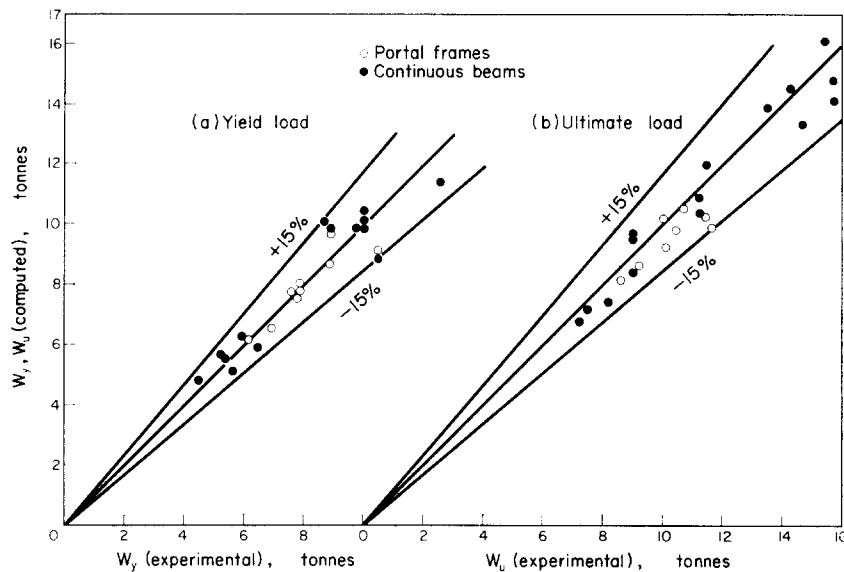


Fig. 25. Comparison of the computed and experimental yield and ultimate loads with test results.

in the diagram indicates the deflection-response of the redundant structure. With the formation of the first hinge, the stiffness of the structure is reduced, there is a physical change in the deformational response of the whole structure and the deflections, increase at a higher rate with increase in load and this is shown by a less steep second straight line in the log-log plot. The first kink, or the junction of the first and second straight lines, hence indicates the load at which the first plastic hinge formed (W_y) and the second straight line indicates the load-deflection response after the formation of first plastic hinge. With the formation of the second plastic hinge, the structure becomes a mechanism and hence deforms with no further increase in load. This is indicated by the third straight line in the log-log plot which is almost parallel to the log deflection axis. The second kink which is the meet of the second and third straight lines indicates the actual stage at which the second critical section reached its ultimate moment, the second (and final)

experimental values of W_y and W_u for the tested portal frames and continuous beams. The satisfactory agreement which is noticed supports the assumption made in the computation of W_y and W_u .

CONCLUSION

Confinement of concrete in steel binders induces a ductile behaviour which results in many benefits for reinforced concrete structures. These have been realized so far only qualitatively. This investigation has resulted in methods of defining the confinement quantitatively and in computing the resisting moment and curvature of reinforced concrete sections having confinement. The proposed method can be used for designing the confinement needed for a section to develop a required curvature. Charts suitable for making such designs have been prepared [19] and will be published in due course.

Table 6. Computed and experimental yield and ultimate loads.

Frame or beam number	Load at yield			Load at ultimate		
	Computed (tonnes)	Experimental (tonnes)	Comp. Expt.	Computed (tonnes)	Experimental (tonnes)	Comp. Expt.
<i>Portal frames</i>						
P0	8.68	8.81	0.985	9.25	10.10	0.924
PA0	9.14	10.47	0.875	9.80	10.47	0.938
P1	6.20	6.16	1.007	8.15	8.55	0.965
PA1	7.80	7.24	1.030	10.23	10.00	1.023
PB1	6.53	6.92	0.944	8.58	9.20	0.935
P2	7.55	7.76	0.973	9.90	11.63	0.852
PA2	7.82	7.84	1.000	10.30	11.45	0.900
PB2	8.02	7.85	1.020	10.55	10.70	0.986
<i>Continuous beams</i>						
CB1	4.82	4.47*	1.080	8.47	9.00	0.940
CB1A	6.30	5.96	1.060	9.70	9.00	1.080
CB1B	5.94	6.46	0.920	9.52	9.00	1.060
CB2	9.90	10.00	0.990	14.17	15.75	0.900
CB2A	9.90	9.77	1.013	14.84	15.75	0.943
CB2B	10.15	10.00	1.015	14.55	14.25	1.020
CB3	8.86	10.47	0.850	13.36	14.63	0.913
CB3A	11.46	12.59	0.910	16.16	15.40	1.048
CB3B	10.50	10.00	1.050	13.90	13.50	1.030
CB4	5.12	5.62	0.912	6.82	7.20	0.947
CB4A	5.55	5.37	1.030	7.20	7.50	0.960
CB4B	5.68	5.25	1.080	7.40	8.18	0.905
CB5	9.90	8.91	1.110	10.40	11.25	0.925
CB5A	10.10	8.71	1.160	12.00	11.44	1.050
CB5B	9.88	8.91	1.110	10.90	11.20	0.973
Average values			0.995			0.966

* Only this value was determined from log load-log curvature diagram.

REFERENCES

1. G. WINTER, Whither inelastic design, *Flexural Mechanics of Reinforced Concrete. Proc. of the Int. Symp.* Miami, Fla. (Nov. 10-12, 1964) p. 581. Am. Soc. of Civ. Engrs. ASCE 1965-50 and ACI SP-12 (1965).
2. F. E. RICHART, A. BRANDTZAEG and R. L. BROWN, A study of failure of concrete under combined compressive stresses. Bull. No. 185. Univ. of Ill. Engg. Expt. Station (1928).
3. G. G. BALMER, V. JONES and D. MCHENRY, Shearing strength of concrete under high triaxial stress—computation of Mohr's envelope as a curve. Structural Research Laboratory, Report No. SP-23, Bureau of Reclamation (1949).
4. F. E. RICHART, A. BRANDTZAEG and R. L. BROWN, The failure of plain and spirally reinforced concrete in compression. Bull. No. 190. Univ. of Ill. Engg. Expt. Station (April 1929).
5. C. W. MARTIN, Spirally prestressed concrete cylinders. *J. Am. Concr. Inst.* **65**, 837 (1968).
6. W. W. L. CHAN, The ultimate strength and deformation of plastic hinges in reinforced concrete frameworks. *Mag. Concr. Res.* **7**, 121 (1955).
7. T. SZULCZYNSKI and M. A. SOZEN, Load-deformation characteristics of concrete prisms with rectilinear transverse reinforcement. Structural Research No. 224, Civil Engg. Studies, Univ. of Ill. (Sept. 1961).
8. H. RÜSCH and S. STÖCKL, *The Effect of Stirrups and Compression Reinforcement on the Flexural Compression Zone of Reinforced Concrete Beams.* No. 148 Deutscher Ausschuss für Stahlbeton, Berlin (1963) (in German).
9. H. E. H. ROY and M. A. SOZEN, A model to simulate the response of concrete to multi-axial loading. Structural Research No. 268. Civil Engng. Studies, Univ. of Ill. (June 1963).

10. H. E. H. ROY and M. A. SOZEN, Ductility of concrete. *Flexural Mechanics of Reinforced Concrete. Proc. of the Int. Symp.* Miami, Fla. (Nov. 10–12, 1964) p. 213. Am. Soc. of Civ. Engrs. ASCE 1965–50 and ACI SP-12 (1965).
11. V. V. BERTERO and C. FELIPPA, Discussion on ductility of concrete. *Flexural Mechanics of Reinforced Concrete. Proc. of the Int. Symp.* Miami, Fla. (Nov. 10–12, 1964) p. 227. Am. Soc. of Civ. Engrs. ASCE 1965–50 and ACI SP-12 (1965).
12. M. T. H. SOLIMAN and C. W. YU. The flexural stress-strain relationship of concrete confined by rectangular transverse reinforcement. *Mag. Concr. Res.* **19**, 223 (1967).
13. A. L. L. BAKER and A. M. N. AMARKONE, Inelastic hyperstatic frame analysis. *Flexural Mechanics of Reinforced Concrete. Proc. of the Int. Symp.* Miami, Fla. (Nov. 10–12, 1964) p. 85. Am. Soc. of Civ. Engrs. ASCE 1965–50 and ACI SP-12 (1965).
14. W. G. CORLEY, Rotational capacity of reinforced concrete beams. *J. Str. Div. Proc. ASCE* **92**, 121 (1966).
15. G. D. BASE, Helical reinforcement in the compression zone of concrete beams. *Conc. and Constl. Engg. (London)*, **57**, 456 (1962).
16. G. D. BASE and J. B. READ, Effectiveness of helical binding in the compression zone of concrete beams. *J. Am. Concr. Inst.* **62**, 763 (1965).
17. J. WARWARUK and A. L. WARD, Effect of confinement of concrete on the behaviour of prestressed concrete beams. *Conference Preprint 501, Structural Engg. Conf.* Seattle, Washington, ASCE (8–12 May 1967).
18. E. G. NAWY, R. F. DANESI and J. J. GRSKO. Rectangular spiral binders effect on plastic hinge capacity in reinforced concrete beams. *J. Am. Concr. Inst.* **65**, 1001 (1968).
19. K. NAGI REDDY, Studies on the behaviour of confined concrete and its application in flexure of reinforced concrete structures. Ph.D. Thesis, Indian Institute of Science, Bangalore (1969).
20. K. T. SUNDARA RAJA IYENGAR, PRAKASH DESAYI and K. NAGI REDDY, Stress-strain characteristics of concrete confined in steel binders. *Mag. Concr. Res.* **22**, 173 (1970).
21. K. T. SUNDARA RAJA IYENGAR, PRAKASH DESAYI and K. NAGI REDDY, Flexure of reinforced concrete beams with confined compression zones. *J. Am. Concr. Inst.* **68**, 719 (1971).
22. M. REINER, *Encyclopedia of Physics. Vol. 6 Elasticity and Plasticity* (Editor FLÜGGE, S.). Springer, Berlin. Chapter on Rheology by Reiner (1958).

Les caractéristiques tension-contrainte du béton confiné en gaines d'acier ont été déterminées. Un nouveau facteur, "l'indice de confinement" a été introduit pour la mesure quantitative du confinement puis, utilisant ces résultats, un "bloc de tension" a été élaboré. Des essais ont été faits sur des poutres en béton armé, à support simple et gaines de confinement hélicoïdales puis analysées sur la base du bloc de tension suggéré. Des essais ont également été faits sur des cadres de portail en béton armé et des poutres continues avec gaines hélicoïdales de confinement utilisant des sections pouvant donner lieu à la formation de charnières plastiques. Une analyse de ces essais indique qu'une redistribution totale des moments a eu lieu à l'ultime.

Es sind Spannungs-Dehnungseigenschaften von Beton, der in Stahlabspannungen begrenzt ist, ermittelt worden. Es ist ein neuer Faktor "Begrenzungsindex" für eine mengenmäßige Bemessung der Begrenzung eingeführt worden, und mit diesen Ergebnissen ist ein "Spannungsbloc" entwickelt worden. Es wurden Tests an einfach gestützten Stahlbetonbalken mit Spiralenbegrenzungsabspannung vorgenommen und auf Grund des vorgeschlagenen Spannungsblocks analysiert. Es wurden auch Tests an Stahlbetonportalrahmen und Durchlaufträgern mit Spiralenabspannungsbegrenzung in Abschnitten mit möglicher plastischer Gelenkbildung durchgeführt. Eine Analyse dieser Tests zeigt, dass eine vollständige Neuverteilung der Momente zum Schluss stattgefunden hat.